International Journal of Hygiene and Environmental Health 267 (2025) 114588

Contents lists available at ScienceDirect

International Journal of Hygiene and Environmental Health

journal homepage: www.elsevier.com/locate/ijheh

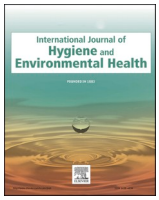

A new approach for simultaneous measurement of aerosol respiratory deposition and its chemical composition: Health risk assessment of metal engineered nanomaterials in consumer spray aerosols

Jinho Lee [a,*], Wei-Chung Su [a,b]

[a] Department of Environmental and Occupational Health Sciences, School of Public Health, University of Texas Health Science Center at Houston, TX, 77030, USA
[b] Southwest Center for Occupational and Environmental Health (SWCOEH), School of Public Health, University of Texas Health Science Center at Houston, TX, 77030, USA

A B S T R A C T

Background: Conventional methods for studying aerosol deposition face limitations when applied to aerosols with irregular shapes and diverse physical properties.
Objective: This study aimed to develop the MALDA (Mobile Aerosol Lung Deposition Apparatus)-MOUDI tandem system to simultaneously estimate the size-specific deposition fraction of aerosols and their chemical constituents. Using this innovative approach, we investigated the respiratory deposition of aerosols generated from selected consumer spray products and evaluated the inhalation risks of engineered nanomaterials (ENMs), specifically metals, in these aerosols.
Methods: Aerosols were generated from two common types of consumer spray products—trigger and propellant sprays. The size-segregated respiratory deposition fraction and mass proportions of target metals in the aerosols were measured. Occupational exposure scenarios were then designed to estimate the non-cancer and cancer risks associated with inhalation of ENMs (metals) in these aerosols.
Results: The MALDA-MOUDI tandem system was successfully developed and validated. Results demonstrated that the non-cancer and cancer risks of inhaled metals due to occupational exposure to the target spray aerosols were below established safety thresholds.
Significance: The MALDA-MOUDI tandem system provides an innovative and systematic approach to assess size-specific aerosol deposition in major human airway regions. This method can be applied to broader environmental and occupational aerosol exposure research to evaluate health risks from toxic substances in aerosols. Findings from this study also offer valuable insights for environmental and occupational health research and propose an improved method for health risk assessment.

1. Introduction

Engineered nanomaterials (ENMs) have been widely used in consumer spray products for cleaning, coating, and sanitizing due to their unique characteristics. It is well known that aerosol generated from spray products is small enough to remain suspended in the air (Park et al., 2020). Thus, workers who use consumer spray products (e.g., vehicle mechanics, cleaning workers, etc.) inevitably inhale ENMs in spray aerosols. Published studies reported that inhalation of some ENMs could lead to adverse health effects on users' respiratory systems (Rossi et al., 2010; Saber et al., 2013; NIOSH, 2014).

To correctly assess the health risk caused by exposure to aerosol and its chemical constituents, the key step is obtaining data on their respiratory deposition. Due to its necessity, several experimental methods for estimating aerosol respiratory deposition were developed. However, these conventional methods required designated radioactive laboratory facilities or collected aerosol deposited in human airway replicas in time-consuming and labor-intensive ways (Su and Cheng, 2006; Zhou and Cheng, 2005; Cheng et al., 1993; Cohen and Asgharian, 1990; Lin et al., 2001). Furthermore, previous experiments conducted with human airway replicas only possessed a few airway generations in the upper tracheobronchial (TB) airways due to the technical challenge of making human lower airway replicas (Smith et al., 2001; Su and Cheng, 2015). As a result, the acquired data were not considered useful because most lung problems caused by aerosol occur in the lower airways, and the application of the aerosol respiratory deposition data is limited (Brown et al., 2002; Geys et al., 2006; Oberdörster et al., 2005). Due to these limitations in the experimental approach, some aerosol respiratory deposition studies were conducted using theoretical models based on theoretical simulations or calculations (Behera et al., 2015; National Committee on Radiation Protection, 1997; Kim et al., 2019; Liu et al., 2020; Park et al., 2018; Rovelli et al., 2020; Schiller et al., 1986; Schiller et al., 1988). However, though complicated theoretical models, such as the International Commission on Radiological Protection (ICRP) model

* Corresponding author. Boston University, School of Public Health, Department of Environmental Science, Talbot W Building, 715 Albany Street, Boston, MA, 02118, USA.
E-mail address: jinholee@bu.edu (J. Lee).

https://doi.org/10.1016/j.ijheh.2025.114588
Received 1 February 2025; Received in revised form 15 April 2025; Accepted 24 April 2025
Available online 27 April 2025

or Multi-Path Particle Dosimetry (MPPD) model, can estimate the deposition of particles, its application is limited as well, since they assume the particles have an ideal shape such as sphere or rod, and have solid phase (International Commission on Radiological Protection, 1994; Miller et al., 2016).

Hence, the conventional methods have difficulties acquiring accurate aerosol respiratory deposition data in lower airways, especially for studying aerosol that has non-solid phases or highly irregular morphology. Aerosols generated from commercially available spray products serve as an example, as they consist of a liquid phase and often contain additives, typically metal-based ENMs with irregular shapes caused by aggregation or agglomeration. Due to these limitations, only a few experimental studies have been conducted to examine the respiratory deposition of spray aerosol and the risks associated with inhaling the ENMs it contains, with most relying instead on theoretical models of aerosol respiratory deposition (Lechasseur et al., 2019; Manigrasso et al., 2015; Son et al., 2020; Sosnowski and Kramek-Romanowska, 2016).

To acquire more useful aerosol respiratory deposition data covering all major airway regions (upper and lower airways), a Mobile Aerosol Lung Deposition Apparatus (MALDA) was developed. The MALDA consists of realistic nasal and oral airway replicas, a TB airway replica down to the 11th lung generation, and a representative alveolar region. MALDA was designed to obtain aerosol respiratory deposition data for the entire human airways from the head airways to the alveoli region (Su et al., 2019, 2021a, 2021b). It was proved that the previous version of MALDA could readily and systematically acquire the respiratory deposition data for ultrafine particles such as 3D printing emission and passive vaping-related e-cigarette aerosol(Su et al., 2019, 2021a, 2021b) (Su et al., 2019, 2021a, 2021b). However, the aerosol generated from consumer spray products has a wide range of diameter, that can reach to micrometer range (Losert et al., 2014; Park et al., 2017), and the approach with the previous version of MALDA (Nano-MALDA, hereafter) is limited.

To overcome this limitation, in this study, a new version of MALDA suitable for aerosol in micrometer size (Micro-MALDA, hereafter) was built. Additionally, both versions of MALDA were coupled with a commercially available size-segregated aerosol sampling instrument: Micro-orifice Uniform Deposit Impactor (MOUDI). In this way, we made an ideal MALDA-MOUDI tandem system that can directly collect inhaled aerosol that penetrates a certain airway region and acquire the deposited amount of aerosol and its chemical components in a certain airway region, simultaneously. This new approach enables a more simplified and accurate aerosol respiratory deposition experiment to study the respiratory deposited mass for the aerosol and its chemical components of concern.

In this study, we focused on the toxic metals contained in aerosol, generated from consumer spray products. We detailed and analyzed the nature of spray aerosol respiratory deposition and metal composition. By leveraging such information, the metal-associated deposited mass, deposited dose, daily dose, and the health risks of metals caused by using spray products in occupational settings were estimated.

2. Methods

2.1. Micro-MALDA and MALDA-MOUDI tandem system

The experimental data of this study was acquired by the MALDA-MOUDI tandem system, which couples MALDAs (Nano- and Micro-MALDA) and MOUDI (model 110-R; MSP Co., Shoreview, MN, USA). The MALDAs consist of 1) a Human airway system (lung replica with Head and TB airways and alveolar region) and 2) an Aerosol measurement system, to measure the size-specific aerosol deposition in human respiratory tracts. Further details of the Nano-MALDA are described in our previous publications (Su et al., 2019, 2021a).

To develop the Micro-MALDA, we tested two TB airways candidates and three alveolar region candidates, and evaluated which best represents the deposition fraction of micro-to submicrometer-sized aerosol. For TB airways, we assessed TB airway replicas with 3rd bifurcation branches and 5th bifurcation branches. The TB airway replicas were 3D-printed by LulzBot TAZ 6 (Aleph Objects, Inc., Loveland, CO, USA), and made from conductive PLA filament (Proto-pasta, ProtoPlant, Vancouver, WA, USA). The three alveolar region candidates (A: High-deposition, B: Mid-deposition, C: Low-deposition) were made of conductive porous foams (W × L = 15.2 cm × 15.2 cm), having different combinations of pore densities (Pore per inch, PPI) and thicknesses (A: 5.080 cm (20 PPI) + 1.905 cm (60 PPI), B: 5.715 cm (20 PPI) + 1.270 cm (60 PPI), and C: 6.350 cm (20 PPI) + 0.635 cm (60 PPI)).

We validated the Micro-MALDA, by comparing the deposition fractions obtained from them to the ICRP aerosol deposition model (International Commission on Radiological Protection, 1994). We used polystyrene latex (PSL) beads (Thermo Fisher Scientific, Inc., Waltham, MA, USA) with diameters ranges 0.5–5.0 μm, since the ICRP model was developed based on the assumption that the aerosol in interest has spherical shape and solid. We dispersed these test particles in distilled water and their aerosol were generated by a nebulizer. The generated droplet passed a diffusion dryer to remove the water portion prior to being delivered to a stainless steel chamber (60 cm × 60 cm × 60 cm). A fan was installed inside the chamber to establish a well-mixed state of the aerosol inside the chamber.

To estimate the deposition fraction acquired from the Micro-MALDA, we modified and utilized the method that we previously used for deposition fraction measurements with Nano-MALDA (Su et al., 2019, 2021a). In the experimental procedure, we first measured the size-dependent concentration of the test aerosol at the inlet of the Micro-MALDA before they entered the head airway ($C_{o,d}$). Then, we measured the size-dependent concentrations of aerosol at the ends of the Head and TB airways ($C_{Head+TB,d}$), and the alveolar region ($C_{Alv,d}$). In this study, we utilized the aerodynamic particle sizer (APS, Model 3321, TSI Inc., Shoreview, MN, USA) that has a measurement range of 0.5–20 μm, as an aerosol measurement system of Micro-MALDA.

Based on the size-dependent concentration of the test aerosol, the size-dependent penetration efficiencies and the deposition fraction of the test aerosol were calculated for the corresponding airway regions. The respiratory deposition fraction, DF (presented as a proportion from 0 to 1.0), obtained from Micro-MALDA is particle size-dependent (d) and airway section-dependent (Head + TB, or Alveolar region), was calculated by following equations:

$$DF_{Head+TB,d} = 1 - \left(C_{Head+TB,d} \;/\; C_{o,d}\right), \tag{1}$$

$$DF_{Alv,d} = \left(C_{Head+TB,d} \;/\; C_{o,d}\right) - \left(C_{Alv,d} \;/\; C_{o,d}\right), \tag{2}$$

$$DF_{Total,d} = DF_{Head+TB,d} + DF_{Alv,d}, \tag{3}$$

where $C_{o,d}$, $C_{Head+TB,d}$ and $C_{Alv,d}$ are number concentrations of aerosol with particle diameter d (particle size distribution) measured by the APS at four sampling locations on Micro-MALDA. $DF_{Head+TB,d}$ and $DF_{Alv,d}$ are the calculated deposition fractions in the head and TB airways, and the alveolar region, respectively.

With this approach, we compared the performance between two TB airway replica candidates and three alveolar region candidates, and chose the candidate for each airway, with one with the best alignment against the reference model. Since the test aerosols used in this study have spherical and solid phases, it is hypothesized that the aerosol respiratory deposition fraction acquired from the number concentration ratio in each airway is the same as the reference ICRP model, which is also designed for spherical solid aerosol. After the evaluation tests, the obtained regional deposition fractions ($DF_{Head+TB,d}$ and $DF_{Alv,d}$), as well as the entire human airway ($DF_{Total,d}$) were compared and determined their homogeneity. The schematic of the validated Micro-MALDA is represented in Fig. 1.

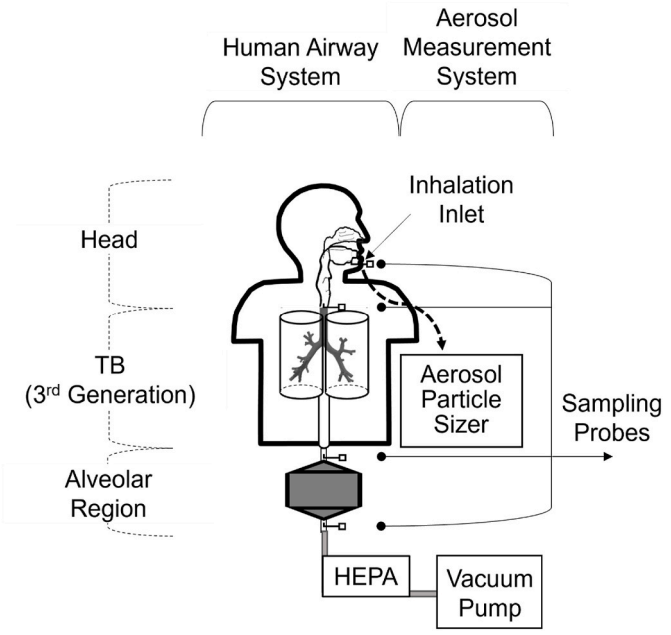

Fig. 1. Schematic diagram of the Micro-MALDA.

To validate the MALDA-MOUDI tandem approach, three experiments with different integrated airway sections were required per each MALDA, to obtain the penetrated mass (*PM*) for calculating the deposited mass (*DM*) in the major human airway regions (Fig. 2). The first experiment was conducted using only MOUDI, without the MALDA, to obtain the size-segregated mass of the original aerosol before inhalation ($PM_{o,d}$). The second experiment was conducted with MOUDI and Head+TB airways of MALDA, to obtain the size-segregated mass of the aerosol penetrated through the head and TB airways ($PM_{Head+TB,d}$). The third experiment was conducted with MOUDI and MALDA with complete human airways, to obtain the size-segregated mass of the aerosol penetrated through the entire human respiratory tracts ($PM_{Head+TB+Alv,d}$).

Based on the size-segregated *PM* obtained from the experiment, the size-segregated *DM* in the head and TB airways, and the alveolar region ($DM_{Head+TB,d}$, and $DM_{Alv,d}$, respectively) was calculated according to the equations below.

$$DM_{Head+TB,d} = PM_{o,d} - PM_{Head+TB,d}, \quad (4)$$

$$DM_{Alv,d} = PM_{Head+TB,d} - PM_{Head+TB+Alv,d}, \quad (5)$$

$$DM_{Total,d} = DM_{Head+TB,d} + DM_{Alv,d}, \quad (6)$$

The deposited mass estimated by Eqs. (4)–(6) represents the mass of the aerosol deposited in a specific airway region by particle size (d). In this approach, we acquired the deposition fraction of the aerosol, by dividing the deposited mass in particular airways ($DM_{Head+TB,d}$; $DM_{Alv,d}$) by the total mass of the generated aerosol ($PM_{o,d}$).

We generated the test aerosols in the same exposure chamber to easily and efficiently control the concentration of aerosol, since the particle size distribution and the concentration of the test aerosol had to be maintained constant. For the validation, we used the same PSL beads, that were used for the Micro-MALDA validation, and NaCl particles (<0.4 μm). Similar to the Micro-MALDA validation process, we dispersed/dissolved these PSL/NaCl test particles in distilled water and generated the aerosol by a nebulizer and aerosol atomizer (3079A, TSI Inc., Shoreview, MN, USA), respectively. The generated droplet passed a diffusion dryer to remove the water portion prior to being delivered to a stainless steel chamber. For micro-to submicrometer-sized aerosol (0.5–5.0 μm), we connected Micro-MALDA and MOUDI and generated PSL aerosol, and for submicrometer-to ultrafine-sized aerosol (<0.4 μm), we connected Nano-MALDA and MOUDI and generated NaCl aerosol. The aerosol was collected onto 37 mm Polytetrafluoroethylene (PTFE) membrane filters (R2PJ037, PALL Co., Port Washington, NY, USA), and the size-segregated aerosol mass was acquired by gravimetric analysis, with a microbalance (CAHN-35, ThermoFisher, Waltham, MA, USA).

To determine whether the deposition fraction is affected by measurement methods, we compared results obtained using the MALDA-MOUDI approach (deposition fractions based on aerosol mass) with those obtained using MALDA and direct-reading instruments (deposition fractions based on aerosol number), which had been previously validated. We used Scanning Mobility Particle Sizers (NanoScan 3910, TSI Inc., Shoreview, MN, USA) to measure the respiratory deposition fraction of submicrometer to ultrafine aerosols (<0.4 μm), and used an APS to measure the respiratory deposition fraction of micro to submicrometer size aerosols. Additionally, the deposition fraction acquired from the MALDA-MOUDI tandem system was also compared to our reference (ICRP) model. After the validation of the Micro-MALDA and MALDA-MOUDI tandem system, we utilized them for the estimation of the spray aerosol deposition and risk assessment of ENMs in it.

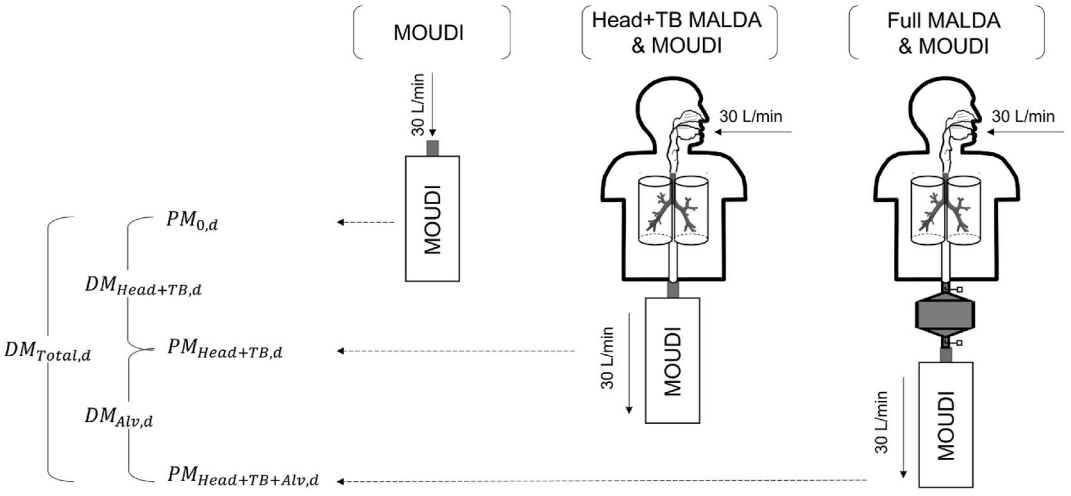

Fig. 2. Schematic diagram of the MALDA-MOUDI tandem system. Penetrated mass (***PM***) and Deposited mass (***DM***) to be acquired from repeated experiments with each stage of the system.

2.2. Test spray products

We used two types of commercially available consumer spray products. Considering the sales volume and homogeneity of contained EMN (in this study, TiO_2), one trigger (hand pump) type (CMX Ceramic Spray Coating 01024, Mothers, CA, USA) spray and one propellant-type spray (VHT Engine Metallic SP403, Speco Thomas, Australia) were selected as the test products. The containing ENMs were determined based on the Safety Data Sheet (SDS) of each product provided by the manufacturers and the statement in the advertisement.

2.3. Respiratory deposition experiments

Laboratory experiments were conducted to study the physical and chemical characteristics of ENM metal-containing aerosol generated from different consumer sprays. Since the products we purchased are designed to be used on the surface, the aerosol was sprayed into the stainless steel chamber through an injection port toward the inner wall of the chamber, which is opposite the injection port (Fig. 3). The settings of the chamber were the same as the settings that we used for the development and validation of Micro-MALDA and MALDA-MOUDI tandem system. The temperature and %RH in the chamber were maintained at 20–25 °C and 50 ± 10 % RH, as recommended as the ideal indoor air condition (American Society of Heating and Refrigerating and Air-Conditioning Engineers (ASHRAE), 2023). To obtain hourly occupational exposure information, the aerosol was sprayed into the chamber with a constant generation rate (2 spray/min). The temperature and %RH in the chamber were maintained at 20–25 °C and 50 ± 10 % RH, to represent recommended indoor air condition (American Society of Heating and Refrigerating and Air-Conditioning Engineers (ASHRAE), 2023). After the spray aerosol was mixed inside the chamber, it was delivered to the oral inlet of the MALDA-MOUDI tandem system.

The aerosol was collected and gravimetrically analyzed, as we did for the validation of the MALDA-MOUDI tandem system. To prevent the evaporation of the liquid portion of the aerosol, the collected samples were weighed immediately. Since the spray aerosol was generated manually, the generation rate may vary with each injection. To minimize this error, we normalized the collected aerosol mass by dividing it by the total mass of sprayed aerosol. All respiratory deposition experiments were repeated at least three times to obtain the mean and standard deviation. The human airway system of each MALDA was cleaned with isopropanol alcohol (IPA) every five experiments and was then recoated its inner surface with new silicon oil to ensure the quality of the experiment. The MOUDI was also cleaned with IPA in every experiment to prevent contamination, and we validated the MALDA-MOUDI tandem system, after each cleaning procedure. Along with the mass, the number concentration of spray aerosol was acquired by SMPS and APS, to investigate the aerosol size distribution and deposition fraction based on its number.

2.4. Metal composition analysis

To find out the size-dependent metal composition in spray aerosol, each aerosol sample (filter) was analyzed by ICP-MS (7500ce, Agilent Technology, Palo Alto, CA, USA), with the EPA IO-3 method (U.S. EPA, 1999). A total of 20 metals (Al, Sb, As, Be, Cd, Cr, Co, Cu, Fe, Pb, Mn, Mo, Ni, Se, Ag, Sr, Sn, Ti, V, and Zn) were selected as target metal constituents, based on previous research (Park et al., 2017, 2020; Laycock et al., 2020). For each set of samples, we prepared at least one corresponding blank filter set in the same manner as the filters used for sample collection in each set of experiments. The metal concentration of the samples was adjusted, by subtracting the background metal concentrations of the blank filters from the sample filters. For descriptive data summary, we considered the filter samples as non-detect (N.D.), when the blank-adjusted metal concentrations were below the limit of detection (LOD). The LOD was calculated as three times the standard deviation of the sample blanks. For the statistical analysis, we replaced the N.D. values with LOD divided by the square root of two.

2.5. Respiratory deposited dose estimation of metals in spray aerosol

The hourly deposited dose of a specific metal k in spray aerosol with diameter d ($HDD_{k,d}$, ng/kg-hr) was calculated by the equation below:

$$HDD_{k,d} = \left(\left(DM_{Head+TB,d} + DM_{Alv,d}\right) \times C_{k,d} \times IR\right) \;/\; (BW \times Q \times T), \quad (7)$$

where, $DM_{Head+TB,d}$, and $DM_{Alv,d}$ are size-dependent deposited mass (ng) of spray aerosol in the Head and TB airways, and alveolar region, respectively. $C_{k,d}$ is the size-dependent mass fraction (0–1.0) of a metal k, found in spray aerosol. IR is the human inhalation rate per hour, which is equal to 15 L/min (U.S. EPA, 2011). BW is human body weight, which is 70 kg. Q is the flow rate used for the MALDA-MOUDI experiment (30 L/min). We used a 30 L/min inspiratory flow rate, to represent the minute ventilation rate of male adults in light exercise (National Committee on Radiation Protection, 1997). The T is the experiment time (hr) for each experiment. The $HDD_{k,d}$ was summed up across the size of spray aerosol (d) to determine the hourly size-cumulative deposited dose

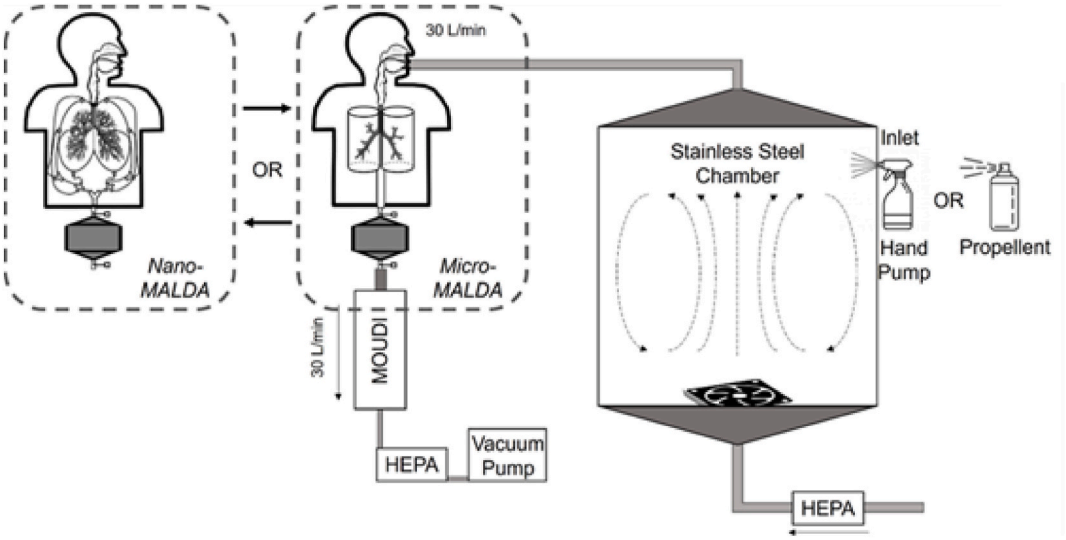

Fig. 3. Schematic diagram of the consumer spray aerosol experiments utilizing MALDA-MOUDI tandem system.

(HDD_k).

2.6. Risk assessment

Non-cancer and cancer risks of metals were assessed based on the estimated average dosage of metal in spray aerosol. With the HDD_k calculated, the average daily dose (ADD_k, ng/kg-day) and the lifetime average daily dose ($LADD_k$, ng/kg-day) were estimated. The average daily dose ADD_k and the lifetime average daily dose $LADD_k$ for a specific metal k was calculated by the following equations:

$$ADD_k = \frac{HDD_k \times CR \times CT}{AT}, \quad (8)$$

$$LADD_k = \frac{HDD_k \times CR \times CT}{LE}, \quad (9)$$

The contact rate (CR), which is the average hour per day that the worker uses the spray product (hr/day), was acquired from the EPA's exposure factor handbook (U.S. EPA, 2011). In this scenario, we assumed that the 95th percentile of the average spray usage hour per day would represent the exposure in the occupational setting. For propellant-type spray, we applied the *exposure time of use* of *aerosol spray paints for cars* (145 min), since the product is designed to paint vehicles. For trigger-type spray, which is designed as a primer and coating spray, we applied the *exposure time of use* of *auto spray primers* (180 min). CT is the contact time, which is the total years that the spray users use the spray product (year), which is the same as the duration of working life, was assumed as 36.5 years (Eurostat, 2023). AT is the average time (year), which is the total year that a worker uses the spray product was also set as 36.5 years. LE is the lifetime expectancy of the worker, which is 70 years. We defined the applicable value on EF as 0.685, which is acquired by dividing the total working days (250 days) in a year (365 days).

The calculated ADD_k and $LADD_k$ were used to estimate the non-cancer health risk by hazard quotient (HQ), acquired by dividing estimated ADD_k s to the reference dose of metal k (RfD_k). We acquired the hazard index (HI), by summing the HQ s of all metals. The lifetime excess cancer risk caused by a specific metal k, CR_k, was calculated by multiplying $LADD_k$ with CSF_k, the cancer slope factor of a specific metal, k. The published RfD and CSF_k or equivalent guidance values for estimating the cancer risk of the target metals were acquired from the EPA Integrated Risk Information System (IRIS), California EPA Office of Environmental Health Hazard Assessment (OEHHA), Agency for Toxic Substances and Disease Registry (ATSDR), and American Conference of Governmental Industrial Hygiene (ACGIH) databases. The HQ_k and HI was considered potential (risk is unacceptable) if they show values higher than 1.0. The lifetime excess cancer risk caused by metal k was considered unacceptable if the calculated cancer risk is higher than 1.0×10^{-6}.

2.7. Data analysis

The descriptive statistics for all collected experimental data, such as the particle size distribution and deposition fraction were calculated and represented. The Bland–Altman method was used to examine the homogeneity of the developed Micro-MALDA and the MALDA-MOUDI tandem system against the ICRP model (Altman and Bland, 1983). In the Bland–Altman analysis, we considered the performance of the Micro-MALDA and MALDA-MOUDI tandem system acceptable when 95 % of the differences between the experimental data and the ICRP data fall within 95 % confidence interval limits (limits of agreement (LOA), hereafter).

Along with the size distributions based on the aerosol's mass and number, mass median diameter (MMD) and count median diameter (CMD) were estimated. The median diameter is defined as the particle size corresponding to the 50th percentile of the aerosol mass or number cumulative distribution curve (Hinds and Zhu, 2022). Since the data was lognormally distributed, the size distributions were log-transformed and fitted as a sigmoidal cumulative distribution curve. The data obtained from different aerosol sizes and different spray types were compared using the Kruskal–Wallis test and the Mann-Whitney U test, respectively. All statistical analyses were completed using R software (v. 4.3.3; R Foundation, Vienna, Austria).

3. Results

3.1. Validation of Micro-MALDA

The validation results of Micro-MALDA are provided in Fig. 4 and Table 1. In the TB airway replica candidate tests, the 3rd bifurcation TB airway replica represented better respiratory deposition than the 5th bifurcation TB airway replica. The deposition data acquired from Head + TB airways with 3rd bifurcation TB showed homogeneity (<5 % of total data are out of the LOA) with a reference model, in all airway sections (Head + TB, Alveolar region, and Total respiratory tract) and represented relatively lower bias than 5th bifurcation TB. Upon the selection of the alveolar region, all three candidates satisfied our criteria for homogeneity analysis. We chose alveolar region B as a final model, based on its low sum of the absolute biases against the reference model.

3.2. Validation of MALDA-MOUDI tandem system

Fig. 5 shows the validation results for the MALDA-MOUDI tandem system. The aerosol respiratory deposition fractions obtained from this system (aerosol mass-based) closely align with the ICRP reference model and a previously validated aerosol number-based approach using MALDA and direct-reading instruments (MALDA-DRI approach, hereafter). We also confirmed that the deposition fraction data from MALDA-MOUDI tandem system fall within the LOA of the ICRP model (Table 2). These findings suggest that both the Micro-MALDA and MALDA-MOUDI tandem system provide reliable aerosol respiratory deposition data.

3.3. Size distribution

The size distribution of spray aerosol was measured by two methods. The number concentration of the spray aerosol was acquired by SMPS and APS, and the data from these two DRIs were fitted and combined by the TSI Data Merge Software (Module 390069, TSI Inc., Shoreview, MN, USA). The mass concentration of the spray aerosol was acquired by MOUDI and gravimetrically analyzed. The number-based size distribution of aerosol generated from the propellant-type spray showed unimodal distributions (Fig. 6a). The peak of the propellant-type spray aerosol was at a diameter of 0.104 μm with a CMD of 0.087 μm. In contrast, the number-based size distribution of aerosol generated from trigger-type spray showed bimodal distributions and peak diameters were 0.120 μm and 1.114 μm. Notably, the number concentration of the aerosol from the propellant-type spray was around 50-fold higher than that of the trigger-type spray. The overall mass-based particle size distributions were unimodal (Fig. 6b). The MMD of the propellant-type spray was 1.660 μm, and the MMD of the trigger-type spray was 1.702 μm. The amount of aerosol generated from the propellant spray was significantly higher, in both measurement methods ($p < 0.001$)

3.4. Aerosol respiratory deposition fraction

Data shown in 7 are the averaged size-dependent aerosol respiratory deposition fractions of spray aerosol in human head and tracheobronchial airways (Head + TB), and the alveolar region (Alv), obtained by MALDA-DRI approach (aerosol number-based) and MALDA-MOUDI tandem system (aerosol mass-based). The aerosol respiratory deposition data obtained from both methods were close to each other. Moreover, aerosol respiratory depositions exhibited similarities in deposition

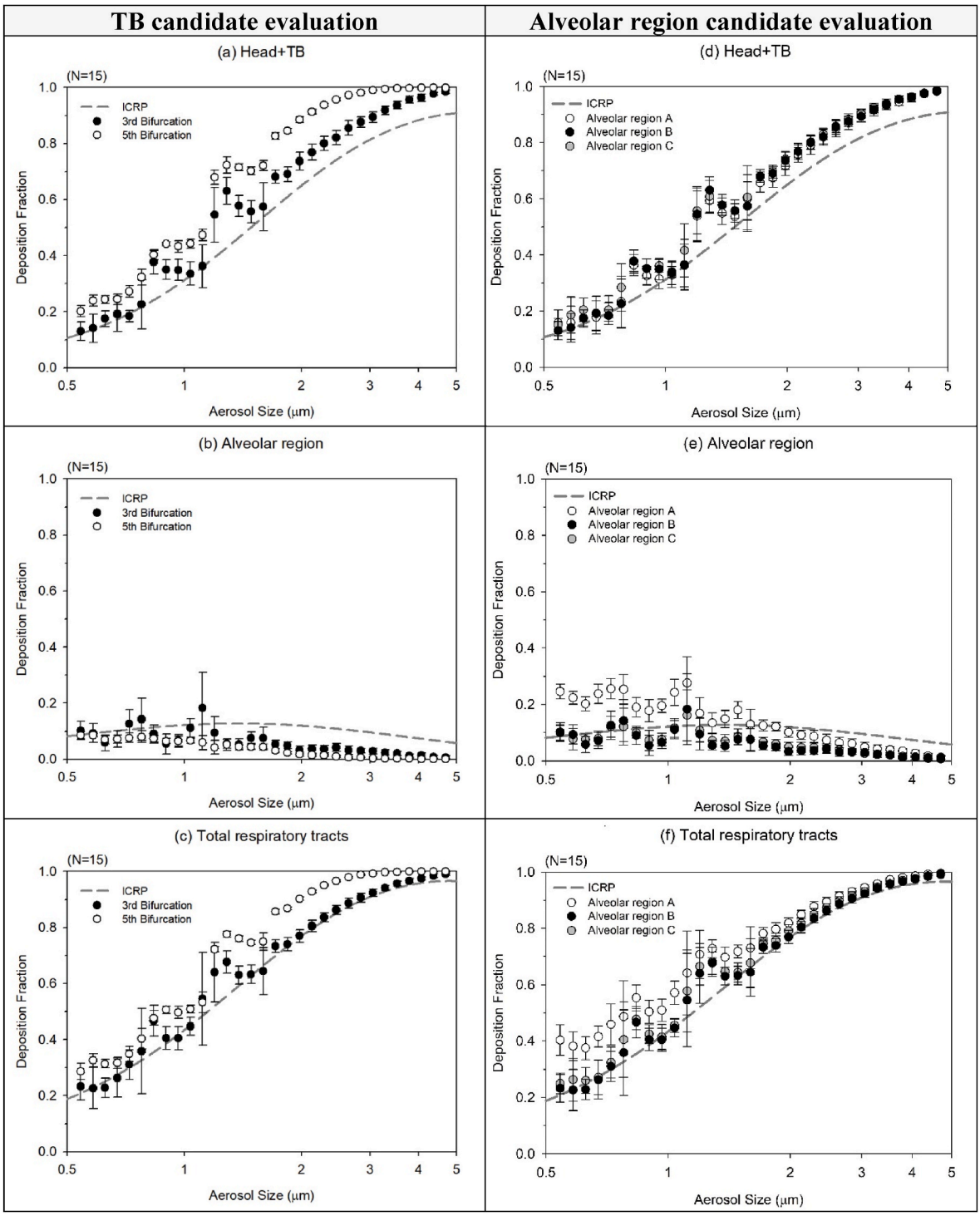

Fig. 4. Aerosol Respiratory deposition fractions of Micro-MALDA with 5th bifurcation and 3rd bifurcation TB airway replica and three alveolar region candidates.

patterns unrelated to the type of spray. It is worth noting that the aerosol number-based respiratory deposition generated from the propellant spray (Fig. 7a) showed large uncertainty and deviated from the ICRP model at around the particle size of 3.0 μm (right tail). This discrepancy might be due to the fact that there were almost no spray particles around this size range, which could be proved from the associated particle size distribution data.

3.5. ENM metal composition in spray aerosol

The metal mass is the sum of the mass of six metals (Ti, Cr, Al, Zn, Sn, and Cu) found in the spray aerosol. As mentioned previously, twenty metals were tested to investigate the metal composition in the spray aerosol and six toxic metals had a significant quantity, exceeding the LOD. Both products were advertised as containing TiO_2 as a major additive, and the portion of Ti in both spray products increased gradually by increasing aerosol size. In propellant-type spray, the portion of Ti was increased from 10 to 90 %, when the size of the aerosol increased from

Table 1
Comparison of TB and alveolar region candidates with the ICRP model (N = 5).

Micro-MALDA TB airways replica evaluation[a]							
Respiratory Tracts	TB Branch Bifurcation	Bias	95 % CI		Limit of acceptance		Data out of LOA (%)
					Lower Limit	Upper Limit	
Head + TB	3rd	0.070	(-0.053,	−0.087)	−0.022	0.161	0
	5th	0.163	(-0.139,	−0.187)	0.034	0.292	3.13
Alveolar region	3rd	−0.045	(-0.059,	−0.032)	−0.116	0.025	0
	5th	−0.068	(-0.079,	−0.058)	−0.125	−0.012	3.13
Total	3rd	0.022	(-0.010,	−0.035)	−0.047	0.092	0
	5th	0.094	(-0.077,	−0.122)	−0.001	0.190	6.25
Micro-MALDA Alveolar region evaluation[b]							
Respiratory Tracts	**Alveolar Region**	**Bias**	**95 % CI**		**Limit of acceptance**		**Data out of LOA (%)**
					Lower Limit	**Upper Limit**	
Head + TB	A (High)	0.085	(0.070,	0.101)	0.024	0.147	0
	B (Mid)	0.091	(0.076,	0.106)	0.031	0.151	0
	C (Low)	0.095	(0.077,	0.113)	0.024	0.166	0
Alveolar region	A (High)	0.046	(0.009,	0.083)	−0.099	0.192	0
	B (Mid)	−0.035	(0.050,	0.020)	−0.094	0.025	0
	C (Low)	−0.029	(-0.046,	0.013)	−0.094	0.035	0
Total	A (High)	0.123	(0.089,	0.157)	−0.010	0.256	0
	B (Mid)	0.049	(0.029,	0.068)	−0.028	0.126	0
	C (Low)	0.058	(0.039,	0.076)	−0.014	0.130	0

[a] For the evaluation of the TB airway replicas, we used the alveolar region *B* to make a complete human airway system.
[b] To evaluate alveolar region candidates, the 3rd bifurcation TB (selected as a final model in this study) was used as a pair of three candidates.

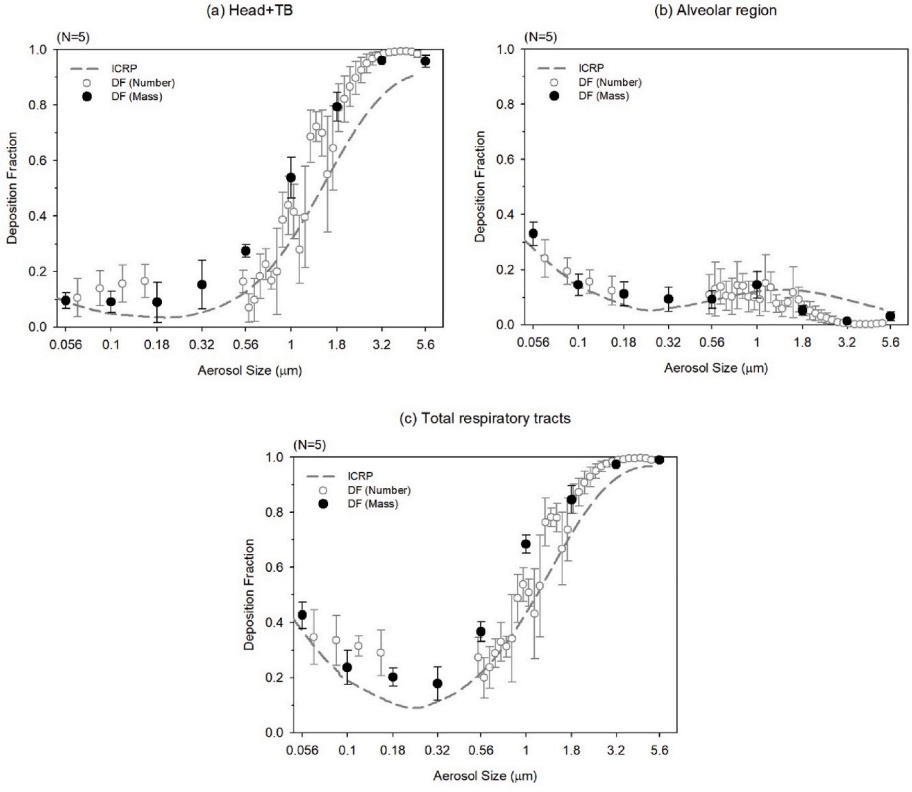

Fig. 5. Aerosol respiratory deposition fractions from the MALDA-MOUDI tandem system (aerosol mass-based), MALDA-DRI approach (aerosol number-based), and ICRP model. (a) Number-based Size Distribution (b) Mass-based Size Distribution.

0.056 to 5.6 μm. Also, in trigger-type spray, the portion of Ti was increased in the range from 1 to 50 %, in aerosol size between 0.056 and 5.6 μm (Fig. 8). The mass ratio of total ENM metal mass to aerosol mass gradually increased with the size of aerosol increases (Fig. 9). For the propellant-type spray, the lowest mass ratio was 1.13×10^{-4} at 0.056 μm, and the highest mass ratio was 0.228 at 5.6 μm. For the trigger-type spray, the lowest mass ratio was 1.77×10^{-3} at 0.10 μm and the highest mass ratio was 0.235 at 3.2 μm. The ratio of total ENM metal mass to aerosol mass was significantly differed by the size of aerosol, in both types of spray ($p < 0.001$).

3.6. Health risk caused by ENM metals presented in spray aerosol

Among the six metals that were identified in the spray aerosol, three of them (Cr, Cu, and Ti) were known to have the potential to induce adverse health effects when inhaled, and the guidance values for their

Table 2
Homogeneity between MALDA-MOUDI tandem system and ICRP model, and MALDA-DRI approach and ICRP model (N = 5).

Respiratory Tracts	Methods	Bias	95 % CI		Limit of acceptance		Data out of LOA (%)
					Lower Limit	Upper Limit	
Head + TB	MALDA-MOUDI (Mass)	0.104	(-0.047,	0.162)	−0.042	0.252	0
	MALDA-DRI (Number)	0.085	(-0.058,	0.112)	−0.089	0.257	0
Alveolar region	MALDA-MOUDI (Mass)	−0.001	(-0.037,	0.036)	−0.093	0.093	0
	MALDA-DRI (Number)	−0.020	(-0.036,	0.005)	−0.117	0.076	0
Total	MALDA-MOUDI (Mass)	0.097	(-0.043,	0.151)	−0.040	0.234	0
	MALDA-DRI (Number)	0.065	(-0.046,	0.083)	−0.051	0.180	7.1

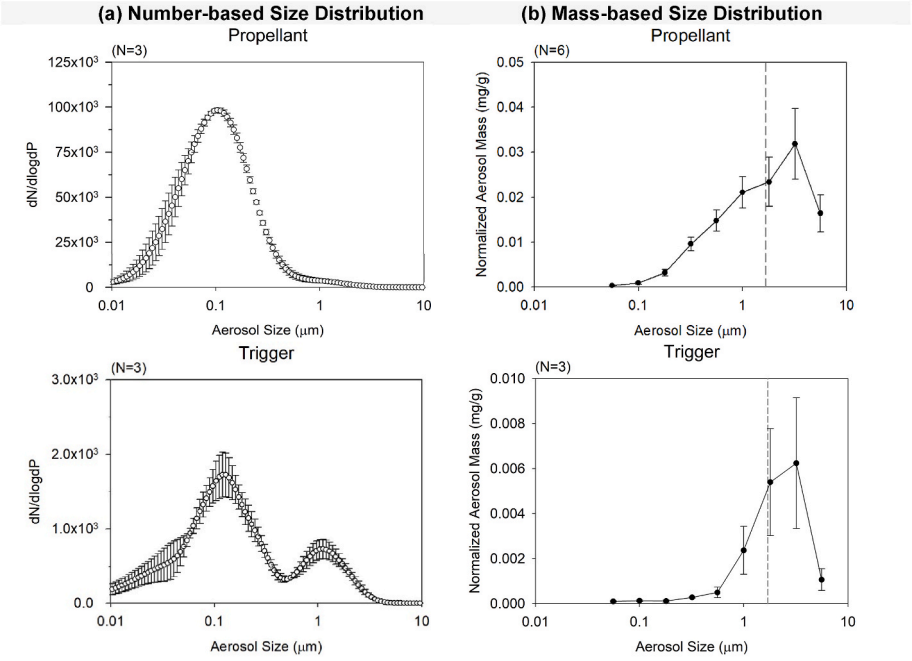

Fig. 6. Particle size distribution of spray aerosol for (a) Number-based size distribution, and (b) Mass-based size distribution. The mass of aerosol was normalized by the mass of the spray liquid used for each experiment. The dashed line on the graph represents the mass median diameter. (a) Propellant (N = 6) (b) Trigger (N = 3).

inhalation toxicity were published by four toxicity databases referred in this study. Therefore, we used these three metals for health risk assessments. Cr(III) and Cu metals are known to have non-cancer toxicity and TiO_2 can cause both non-cancer and cancer effects due to inhalation. However, since no guidance value for TiO_2-related cancer risk was published to the databases we referred, only non-cancer risks were estimated in this study. To estimate the risk of occupational exposure to ENM in consumer spray products, the reference doses (RfDs) were calculated based on the CalEPA REL, ACGIH TLV, and ATSDR MRL. With this toxicity information, as well as the spray aerosol respiratory deposition data and the metal mass ratio data acquired by MALDA-MOUDI experiments, the average daily doses and non-cancer health risks caused by toxic ENM metals present in spray aerosol were estimated. The calculated daily doses and health risks based on the experiments designed in this study are listed in Table 3.

It is worth noting that since the ACGIH has different TLV for finescale TiO_2 particles (2.5 mg/m^3) and nanoscale TiO_2 particles (0.2 mg/m^3), in this study, we assumed that 100 % of the Ti obtained in the spray aerosol samples has a form of nanoscale TiO_2 aerosol, for conservative estimations of the health risk. Since the analytical method that we used in this study only provides the mass of Ti, we converted the mass of Ti to the mass of TiO_2 by multiplying the ratio between their molecular weight. Additionally, we assumed that the entire portion of the total Cr found in the spray aerosol samples was Cr(III), since the analytical method we used only provides the mass of total Cr. Considering the spray aerosol is commonly generated under the normal temperature and inhaled into the human respiratory without additional chemical reactions, it is reasonable to assume that Cr(III), the most common oxidation state of Cr, is less likely to be oxidized and exists as is.

The ENM metal-induced non-cancer risks caused by exposure to occupational use of propellant- and trigger-type spray products were found to be generally acceptable (Table 2). For the propellant-type spray, the *HQ* for Cr(III) was found to be less than 1.0 (1.34×10^{-2}). The *HQ*s for Cu and TiO_2 were also found to be less than 1.0 (1.67×10^{-4} and 2.98×10^{-4}, respectively). The calculated *HI* for exposure to propellant-type spray aerosol was 1.65×10^{-2}, indicating that the non-cancer risks induced by toxic ENM metals present in the propellant-type spray aerosol is overall acceptable (*HI* < 1.0). Likewise, for the trigger-type spray, the calculated *HQ*s of each ENM metal were also generally less than 1.0 (Cr(III): 7.64×10^{-3}, Cu: 1.46×10^{-4}, TiO_2: 4.22×10^{-4}), and the calculated *HI* was 8.21×10^{-3}.

4. Discussion

In this study, we developed a new experimental tool, Micro-MALDA, and MALDA-MOUDI tandem system for improved aerosol respiratory deposition experiments. By applying this new approach, the respiratory deposition of metal in spray aerosol and metal-induced health risks were assessed.

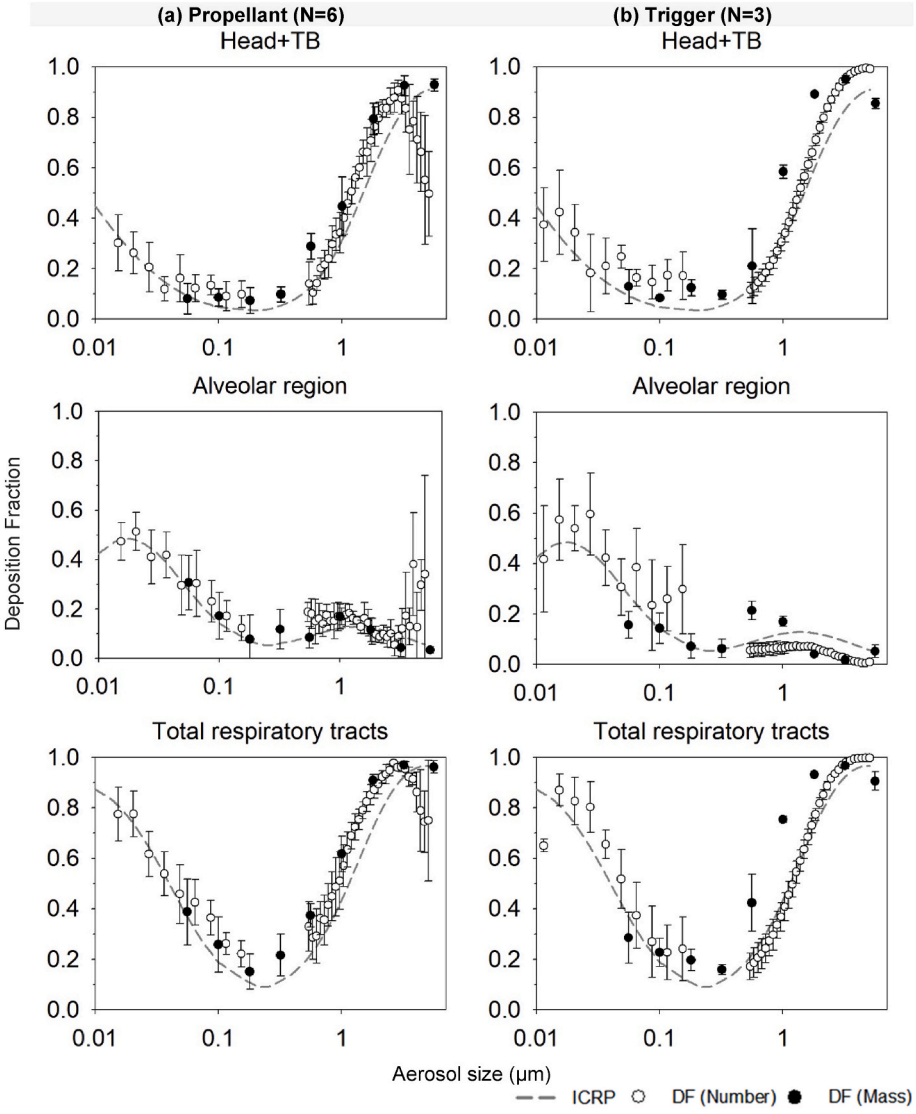

Fig. 7. Respiratory deposition fractions of spray aerosol. (a) Propellant-type sprays, and (b) trigger-type sprays. (a) Propellant (b) Trigger.

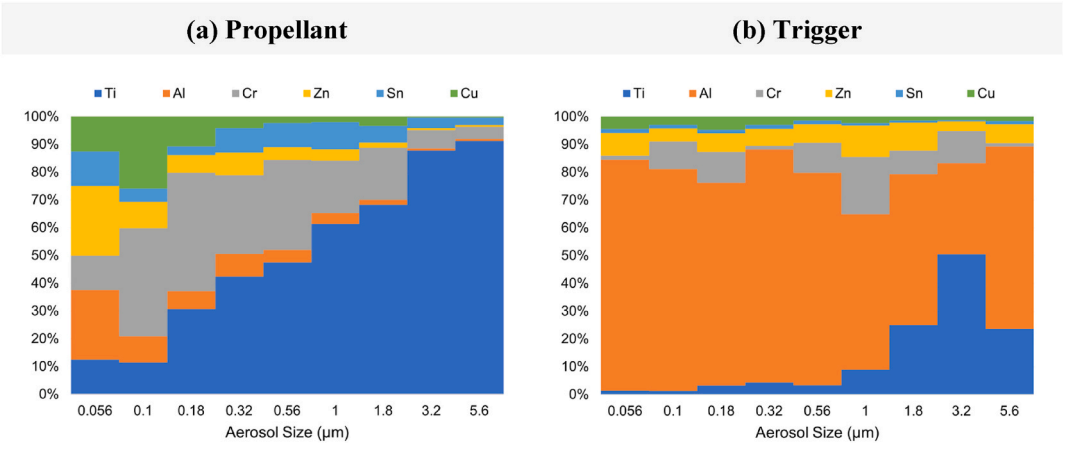

Fig. 8. Size-dependent ENM metal ratio in consumer spray aerosol in (a) propellant-type sprays and (b) Trigger-type sprays.

4.1. Micro-MALDA and MALDA-MOUDI tandem system

To our knowledge, the Micro-MALDA is the first experimental tool designed to estimate the respiratory deposition of micrometer-sized aerosols across the entire (upper and lower) respiratory tract. Most studies have used only extrathoracic (Head and upper TB) human

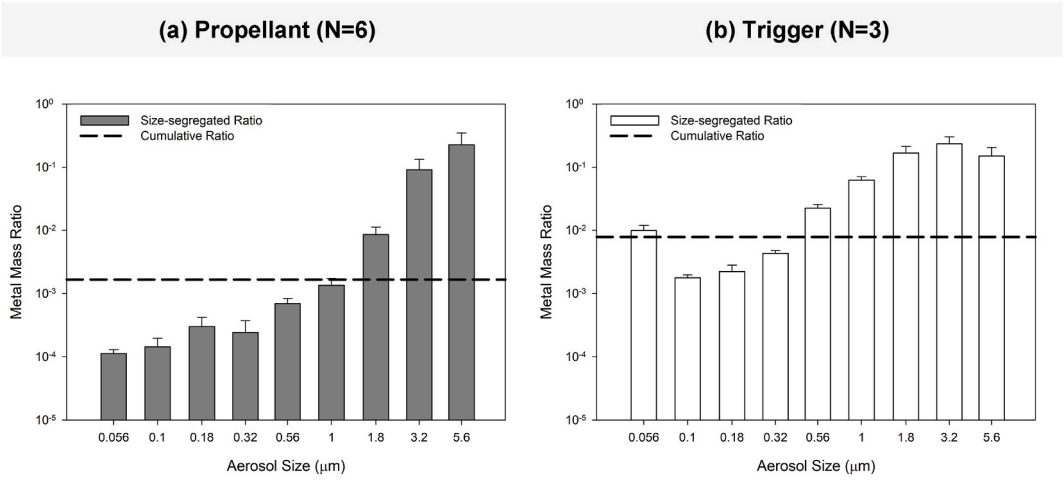

Fig. 9. Size-dependent metal mass ratio in spray aerosol for (a) propellant-type sprays and (b) trigger-type sprays.

Table 3
Health risks caused by ENM metals present in spray aerosol generated by (a) propellant-type spray, and (b) trigger-type spray.

(a) Propellant				
	Cr(III)[a]	Cu	TiO_2	
ADD[b]	0.021	0.005	0.184	
HQ	1.34×10^{-2}	1.67×10^{-4}	2.98×10^{-3}	HI: 1.65×10^{-2}
(b) Trigger				
	Cr(III)[a]	Cu	TiO_2	
ADD[b]	0.012	0.005	0.026	
HQ	7.64×10^{-3}	1.46×10^{-4}	4.22×10^{-4}	HI: 8.21×10^{-3}
RfD[b]	1.5429[c]	30.857[$]	61.714[§]	

[a] The proportion of Cr(III) was assumed to be 100 % of the total Cr detected.
[b] The unit of ADD and RfD is μg/kg·day.
[c] ATSDR. $: CalEPA. §: ACGIH.

airway replica (Zhou and Cheng, 2005; Ahookhosh et al., 2019; Borojeni et al., 2014; Golshahi et al., 2012; Grgic et al., 2004; Inthavong et al., 2010; Kelly et al., 2004; Lim et al., 2021; Lizal et al., 2012; Storey-Bishoff et al., 2008; Verbanck et al., 2016; Zhou et al., 2013), often overlooking aerosol respiratory deposition in the lower TB and alveolar regions. Furthermore, unlike the previous studies that made replicas using glass or metal casts (Bickmann et al., 2008; DeHaan and Finlay, 2001; Kim and Fisher, 1999), the Micro-MALDA is made of plastic, making it suitable for studies requiring mobility.

Moreover, the MALDA-MOUDI tandem system is the first experimental method that can simultaneously obtain the mass of aerosol deposited in respiratory tracts and its chemical composition. In our previous study, we assessed health risks caused by inhaling chemicals in the aerosol by obtaining respiratory deposition data with DRIs and aerosol chemical composition using a cascade impactor (Su et al., 2024). However, DRIs often operate within different size ranges compared to size-segregated aerosol samplers. The MALDA-MOUDI tandem system prevents inaccuracies that may arise from extrapolating data across varying size ranges, as seen in such studies. In addition, compared to studies that acquired aerosol respiratory deposition using theoretical model, such as the ICRP or MPPD model (Rovelli et al., 2020; Can-Terzi et al., 2021; Chalvatzaki et al., 2018; Long et al., 2021; Voliotis et al., 2021; Wang et al., 2019), the MALDA-MOUDI tandem system does not rely on the assumption of the shape and physical properties of the aerosol.

4.2. Size distribution

As shown in Fig. 6, the number-based size distribution of spray aerosol represented an unimodal shape in propellant-type spray. Previous studies on spray aerosol reported similar findings regarding the aerosol number-based size distribution. Notably, several studies also identified a unimodal number-based size distribution in propellant-type spray aerosol, with particle sizes predominantly in the ranges of 0.030–0.100 μm (Park et al., 2020; Losert et al., 2014; Laycock et al., 2020; Chen et al., 2010; Clausen et al., 2023; Nørgaard et al., 2009; Lorenz et al., 2011). This result was similar to the number-based peak diameter found in this study (0.104 μm). On the other hand, the number-based size distribution of trigger-type spray aerosol in this study represented a bimodal shape. Published studies in the literature reported mixed modality (unimodal or bimodal distribution) for trigger-type spray aerosol within the nano-to micrometer size range. Though the reported modality varied by the product, they all had common number-based bimodal peak diameters at 0.200–0.300 μm and 1.0–2.0 μm (Park et al., 2020; Laycock et al., 2020; Quadros and Marr, 2011). These peak diameters were similar to the two peaks found in this study (0.120 μm and 1.114 μm).

Moreover, the MMD (1.660–1.707 μm) and mass-based peak diameter (3.2 μm) acquired from this study were also in comparable ranges as those reported in published studies. For example, in studies that used a cascade impactor to collect spray aerosol samples, the mass-based peak diameters were at a range between 2.0 and 5.6 μm (Laycock et al., 2020; Dua et al., 1995). MMD or peak diameter was also reported to be within equivalent range between this study and the studies that estimated the MMD or mass-based peak diameter by converting the aerosol number concentration (Clausen et al., 2023; Calderón et al., 2017; Pearce et al., 2019).

4.3. Respiratory deposition of spray aerosol

The respiratory deposition of spray aerosol showed similar results across the two spray products (Fig. 7). Although the two spray products used in this study generate liquid aerosols, the resulting respiratory deposition fractions generally follow the ICRP model. This result proves again that aerosol respiratory deposition is mainly a function of particle size (International Commission on Radiological Protection, 1994; Hinds and Zhu, 2022). The deposition fractions obtained in this study generally fall within the range reported by previous studies that used the ICRP model, the MPPD model, or computational fluid dynamics simulations to estimate the respiratory deposition of consumer spray aerosols (Fig. 10). (Park et al., 2018; Tian et al., 2015; Lovén et al., 2019). However, comparing the accuracy of each approach remains challenging due to variations in exposure scenarios across studies, including differences in aerosol physical properties and inhalation rates.

Fig. 7a showed that the number-based respiratory deposition fractions of propellant spray aerosol deviated from the ICRP model

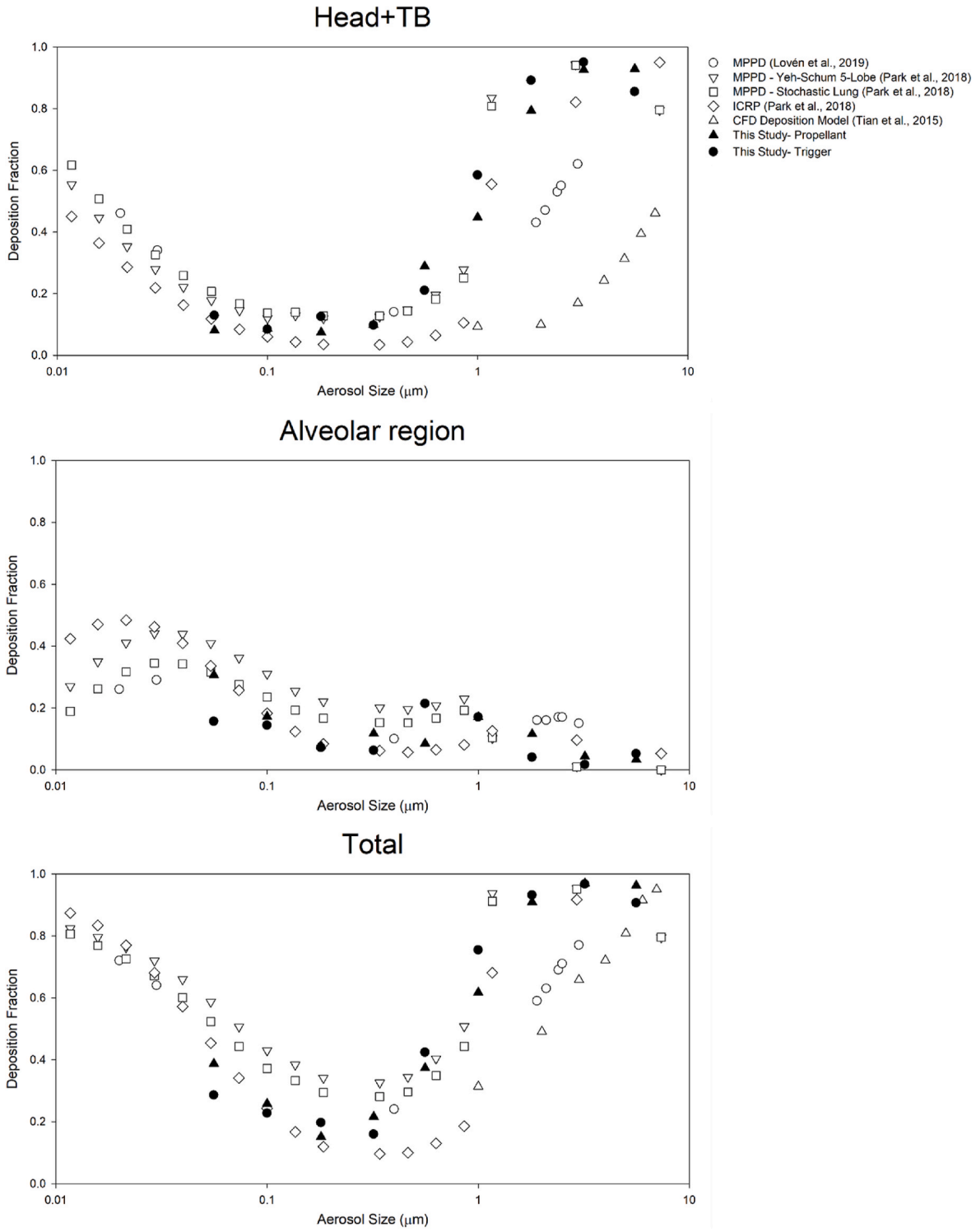

Fig. 10. Deposition fractions of consumer spray aerosols acquired from previous studies and this study.

significantly when the aerosol diameter was larger than 3 μm. The possible reason for this result could be attributed to the low aerosol number concentration in the size range larger than 3 μm, as shown in Fig. 6. Due to the low aerosol concentration in this size range reaching the LOD of the instrument, a higher variation in the measured aerosol concentration was observed, which led to a huge variance in the deposition fraction (Fig. 7a). In contrast, the aerosol generated from trigger-type spray showed an overall close fit compared to the ICRP model, even in the size range larger than 3 μm. This result is due to the fact that the trigger-type spray has the capability to produce a comparatively higher amount of aerosol in the size range exceeding 3 μm.

4.4. ENM metal composition in spray aerosol

It is crucial to consider the size-dependent chemical composition in aerosol for accurately estimating the respiratory deposited mass of specific toxic chemicals in aerosol and thus facilitating a more precise health risk assessment caused by aerosol exposure. To date, several

studies investigated the composition of metal ENMs in spray products, and found known ENMs, such as Ag, Zn, Ti, and their oxides (Park et al., 2020; Nørgaard et al., 2009; Lorenz et al., 2011; Calderón et al., 2017). However, these previous studies only investigated the amount of metal ENMs by removing the solvents of spray aerosol, or acquired the ENM composition in bulk spray liquid or total suspended aerosol. Only a few studies have quantified the size-segregated ENM metal ratio in spray aerosol and estimated the health risk based on this information. Quadros and Marr (2011) investigated the size-segregated silver ENM composition in a trigger-type spray aerosol using a four-stage cascade impactor, and reported that there was no association between the aerosol size and ENM metal mass ratio (Quadros and Marr, 2011). This result is contradictory to what was found in this study, which clearly presented inconsistent metal proportions across the aerosol size (Fig. 9). The reason for the discrepancy between the two studies is not clear immediately; it could be due to the difference in the resolution of the aerosol samplers used in the two studies. The cascade impactor used by Quadros and Marr (2011) had a relatively low resolution (4 stages, 0.25–2.5 μm) compared to MOUDI (11 stages, 0.056–18 μm) used in this study (Quadros and Marr, 2011).

4.5. Health risk of ENM metal in spray aerosol

In the literature, most of the studies regarding consumer spray products are focused on the chemical components in the spray solution, such as volatile organic chemicals. Several studies have investigated the characteristics of ENM metal in spray products. Although some of the published studies quantified the ENM metal composition in spray aerosol and estimated the inhalation dose of spray aerosol, very few of them determine the health risks caused by using consumer spray products (Losert et al., 2014; Park et al., 2017; Laycock et al., 2020; Calderón et al., 2017; Nazarenko et al., 2014). Quadros and Marr (2011) estimated the risk of silver nanomaterial in a finger pump spray product (Quadros and Marr, 2011). The reported *HQ* (non-cancer risk) due to silver nanomaterial was 1/40 for the alveolar inflammatory response and 1/16 for the argyria. Wang et al. (2021) estimated the risk of TiO_2-contained aerosol generated by a sunscreen spray (Wang et al., 2021). The reported range of *HQ* was from 0.07 to 0.23, which is significantly higher than *HQ* acquired from this study (4.22×10^{-4} - 2.98×10^{-3}). However, the reference dose of TiO_2 was the EC_{50} derived from a probabilistic model based on the separated animal dose-response study. Moreover, the estimated daily dose of TiO_2 applied for Wang's study (6.48–63.21 μg) was significantly higher than our study. Therefore, based on the difference in experimental design and methodology, the *HQ*s in Wang's study cannot be directly compared to ours. The health risks estimated in this study are considered unique, which integrated size-dependent aerosol respiratory deposition data and size-dependent chemical composition data and followed the conventional EPA risk assessment method.

4.6. Limitations of the study

The diversity of spray products contributes to a significant variation in aerosol emission characteristics. For example, factors such as the composition of the base (water or an organic solvent) and the design and pressure of the nozzle can influence the aerosol generated aerosol remarkably (Park et al., 2017; Quadros and Marr, 2011; Jung et al., 2021; Nuyttens et al., 2007). Therefore, the consumer spray product tested in this study (one propellant-type spray and one trigger-type spray) can only represent a small portion of the entire spray products on the market.

The environments in which the spray products are used can significantly affect the concentration of the spray aerosol, which will then affect the amount of spray aerosol that the user is exposed to and inhaled. Based on this, the experimental design and setup in this study can only be applied to indoor exposure scenarios with limited ventilation. Since the volume of the chamber used in this study is much smaller than a realistic room or workplace, the concentration of the spray aerosol in the chamber and induced risk were expected to be considerably higher than that in a real environment. Moreover, the results obtained in our study did not account for the factors that may affect metal ENM exposure or induced risks in specific populations. Hence, considering factors such as physical activity, intensity of work and physiological characteristics (inhalation rate and deposition fraction) along with the demographic factors (age and gender), temperature and humidity and other related factors, such as wearing PPE, temperature, and humidity could provide detailed information about the exposure and risk.

Additionally, although we calculated size-segregated deposited doses, our final risk estimates followed conventional risk assessment methods, which are limited in their capacity to account for aerosol-size-specific risks. Given that smaller particles may pose higher risks, this size-aggregated approach may underestimate potential hazards posed by ultrafine or otherwise more bioactive particles, and therefore careful interpretation of these findings is needed.

This study made assumptions regarding estimating the quantity of certain ENM metals in the spray aerosol. First, the amount of TiO_2 in the spray aerosol was predicted based on the amount of Ti detected in the spray aerosol samples. Since the ICP-MS can detect metal elements but not chemical compounds, only Ti was found in the spray aerosol samples. However, it is a reasonable assumption that all Ti detected was from TiO_2 because TiO_2 is the major ingredient in the test spray products. Second, all the detected total Cr was assumed to be Cr(III) and health risks associated with Cr(VI) were not considered in this study. This assumption was based on the fact that the likelihood of the oxidation of Cr(III) to Cr(VI) under normal environments is very low. However, given that the proportion of Cr(VI) and Cr(III) in total Cr in consumer spray products have not been investigated thoroughly, further research is needed. Consequently, the risk identified in this study may vary depending on the aerosol generation process. The above limitations highlight the complexity of conducting a comprehensive risk assessment for aerosol generated from spray products and indicate that results acquired from this study may not universally apply to all cases using spray products. Hence, the outcomes of this study should serve as a reference rather than a comprehensive guide.

5. Conclusion

A new simplified model of human airway systems, Micro-MALDA was developed, for obtaining aerosol respiratory deposition in micrometer size range. The newly developed Micro-MALDA together with the Nano-MALDA was serially connected with MOUDI, to form a MALDA-MOUDI tandem system. The results from the MALDA-MOUDI tandem system validation indicated that the estimated mass-based aerosol respiratory deposition fraction well aligns with the ICRP model. By leveraging this novel approach, the size-segregated metal composition in consumer product spray aerosol and their respiratory deposition data were obtained and used to estimate the deposited mass, daily doses, and health risks caused by the potentially harmful metals in spray aerosol. The estimated non-cancer risks caused by metals in spray aerosol were smaller than the conventional risk criteria, for trigger and propellant type sprays. This research presents a novel method for evaluating the inhalation risks caused by particular chemicals in aerosol (in this study, metals in spray aerosol). Results obtained provide insights into the effect of aerosol physical and chemical characteristics on the respiratory deposited mass of spray aerosol-contained metal substances generated from different type of sprays. However, the estimated risk may vary by the usage topography, the condition of the environment, or the composition of metal and design of spray products. Therefore, it is essential to carefully manage the amount of consumer spray products used and the occupational control methods, such as adequate ventilation and suitable PPE, especially in occupational settings. Findings from this

study contribute to our understanding of the potential health risks associated with the occupational use of spray products with ENM metal, which could inform related policies and interventions to mitigate health risks induced by exposure to spray aerosol.

CRediT authorship contribution statement

Jinho Lee: Writing – original draft, Visualization, Validation, Project administration, Methodology, Investigation, Funding acquisition, Formal analysis, Conceptualization. **Wei-Chung Su:** Writing – review & editing, Supervision, Methodology, Conceptualization.

Conflict of interest

The authors report there are no competing interests to declare.

Acknowledgment

This research was supported by a Research Trainee Awards from the Southwest Center for Occupational and Environmental Health (SWCOEH), under the CDC/NIOSH T42 Educational Resource Center Training Grants (T42OH008421).

References

Ahookhosh, K., Yaqoubi, S., Mohammadpourfard, M., Hamishehkar, H., Aminfar, H., 2019. Experimental investigation of aerosol deposition through a realistic respiratory airway replica: an evaluation for MDI and DPI performance. Int. J. Pharm. 566, 157–172.
Altman, D.G., Bland, J.M., 1983. Measurement in medicine: the analysis of method comparison studies. The Statistician 32 (3), 307.
American Society of Heating, Refrigerating and Air-Conditioning Engineers (ASHRAE), 2023. ASHRAE Standard 55-2023. Thermal Environmental Conditions for Human Occupancy.
Behera, S.N., Betha, R., Huang, X., Balasubramanian, R., 2015. Characterization and estimation of human airway deposition of size-resolved particulate-bound trace elements during a recent haze episode in Southeast Asia. Environ. Sci. Pollut. Res. 22 (6), 4265–4280.
Bickmann, D., Wachtel, H., Kröger, R., Langguth, P., 2008. Examining inhaler performance using a child's throat model. Respir. Drug. Deliv. 2, 565–570.
Borojeni, A.A.T., Noga, M.L., Vehring, R., Finlay, W.H., 2014. Measurements of total aerosol deposition in intrathoracic conducting airway replicas of children. J. Aerosol Sci. 73, 39–47.
Brown, J.S., Zeman, K.L., Bennett, W.D., 2002. Ultrafine particle deposition and clearance in the healthy and obstructed lung. Am. J. Respir. Crit. Care Med. 166 (9), 1240–1247.
Calderón, L., Han, T.T., McGilvery, C.M., Yang, L., Subramaniam, P., Lee, K.B., et al., 2017. Release of airborne particles and Ag and Zn compounds from nanotechnology-enabled consumer sprays: implications for inhalation exposure. Atmos. Environ. 155, 85–96.
Can-Terzi, B., Ficici, M., Tecer, L.H., Sofuoglu, S.C., 2021. Fine and coarse particulate matter, trace element content, and associated health risks considering respiratory deposition for Ergene Basin, Thrace. Sci. Total Environ. 754, 142026.
Chalvatzaki, E., Chatoutsidou, S.E., Mammi-Galani, E., Almeida, S.M., Gini, M.I., Eleftheriadis, K., et al., 2018. Estimation of the personal deposited dose of particulate matter and particle-bound metals using data from selected European cities. Atmosphere 9 (7), 248.
Chen, B.T., Afshari, A., Stone, S., Jackson, M., Schwegler-Berry, D., Frazer, D.G., et al., 2010. Nanoparticles-containing spray can aerosol: characterization, exposure assessment, and generator design. Inhal. Toxicol. 22 (13), 1072–1082.
Cheng, Y.S., Su, Y.F., Yeh, H.C., Swift, D.L., 1993. Deposition of thoron progeny in human head airways. Aerosol. Sci. Technol. 18 (4), 359–375.
Clausen, P.A., Kofoed-Sørensen, V., Jensen, S.P., Larsen, B.X.N., Jensen, A.C.Ø., Frederiksen, M., et al., 2023. Characterization of the aerosol release from spray cleaning and disinfection products – spray scenarios in a climate chamber. Int. J. Hyg Environ. Health 252, 114220.
Cohen, B.S., Asgharian, B., 1990. Deposition of ultrafine particles in the upper airways: an empirical analysis. J. Aerosol Sci. 21 (6), 789–797.
DeHaan, W.H., Finlay, W.H., 2001. *In vitro* monodisperse aerosol deposition in a mouth and throat with six different inhalation devices. J. Aerosol Med. 14 (3), 361–367.
Dua, S.K., Hopke, P.K., Raunemaa, T., 1995. Hygroscopic growth of consumer spray products. Aerosol. Sci. Technol. 23 (3), 331–340.
Eurostat, 2023. Duration of working life [internet] [cited 2024 Dec 19]. Available from: https://ec.europa.eu/eurostat/databrowser/view/lfsi_dwl_a/default/table?lang=en.
Geys, J., Coenegrachts, L., Vercammen, J., Engelborghs, Y., Nemmar, A., Nemery, B., et al., 2006. In vitro study of the pulmonary translocation of nanoparticles. Toxicol. Lett. 160 (3), 218–226.
Golshahi, L., Noga, M.L., Finlay, W.H., 2012. Deposition of inhaled micrometer-sized particles in oropharyngeal airway replicas of children at constant flow rates. J. Aerosol Sci. 49, 21–31.
Grgic, B., Finlay, W.H., Heenan, A.F., 2004. Regional aerosol deposition and flow measurements in an idealized mouth and throat. J. Aerosol Sci. 35 (1), 21–32.
Hinds, W., Zhu, Y., 2022. Aerosol Technology: Properties, Behavior, and Measurement of Airborne Particles, second ed. John Wiley & Sons: New York, NY, USA.
International Commission on Radiological Protection, 1994. Human respiratory tract model for radiological protecction. ICRP publication 66. Vol. 24 (1-3). Oxford, England. Ann. ICRP.
Inthavong, K., Choi, L.T., Tu, J., Ding, S., Thien, F., 2010. Micron particle deposition in a tracheobronchial airway model under different breathing conditions. Med. Eng. Phys. 32 (10), 1198–1212.
Jung, Y., Kim, Y., Seol, H.S., Lee, J.H., Kwon, J.H., 2021. Spatial uncertainty in modeling inhalation exposure to volatile organic compounds in response to the application of consumer spray products. Int. J. Environ. Res. Publ. Health 18 (10), 5334.
Kelly, J.T., Asgharian, B., Kimbell, J.S., Wong, B.A., 2004. Particle deposition in human nasal airway replicas manufactured by different methods. Part I: inertial regime particles. Aerosol. Sci. Technol. 38 (11), 1063–1071.
Kim, C.S., Fisher, D.M., 1999. Deposition characteristics of aerosol particles in sequentially bifurcating airway models. Aerosol. Sci. Technol. 31 (2–3), 198–220.
Kim, Y.H., Tong, Z.B., Chan, H.K., Yang, R.Y., 2019. CFD modelling of air and particle flows in different airway models. J. Aerosol Sci. 134, 14–28.
Laycock, A., Wright, M.D., Römer, I., Buckley, A., Smith, R., 2020. Characterisation of particles within and aerosols produced by nano-containing consumer spray products. Atmos. Environ. X, 100079.
Lechasseur, A., Altmejd, S., Turgeon, N., Buonanno, G., Morawska, L., Brunet, D., et al., 2019. Variations in coil temperature/power and e-liquid constituents change size and lung deposition of particles emitted by an electronic cigarette. Phys. Rep. 7 (10), e14093.
Lim, S.H., Park, S., Lee, C.C., Ho, P.C.L., Kwok, P.C.L., Kang, L., 2021. A 3D printed human upper respiratory tract model for particulate deposition profiling. Int. J. Pharm. 597, 120307.
Lin, T.C., Breysse, P.N., Laube, B.L., Swift, D.L., 2001. Mouthpiece diameter affects deposition efficiency in cast models of the human oral airways. J. Aerosol Med. 14 (3), 335–341.
Liu, X., Kong, S., Yan, Q., Liu, H., Wang, W., Chen, K., et al., 2020. Size-segregated carbonaceous aerosols emission from typical vehicles and potential depositions in the human respiratory system. Environ. Pollut. 264, 114705.
Lizal, F., Elcner, J., Hopke, P.K., Jedelsky, J., Jicha, M., 2012. Development of a realistic human airway model. Proc. Inst. Mech. Eng. 226 (3), 197–207.
Long, L., He, J., Yang, X., 2021. Characteristics, emission sources and health risk assessment of trace elements in size-segregated aerosols during haze and non-haze periods at Ningbo, China. Environ. Geochem. Health 43 (8), 2945–2963.
Lorenz, C., Hagendorfer, H., Von Goetz, N., Kaegi, R., Gehrig, R., Ulrich, A., et al., 2011. Nanosized aerosols from consumer sprays: experimental analysis and exposure modeling for four commercial products. J. Nanoparticle Res. 13 (8), 3377–3391.
Losert, S., Von Goetz, N., Bekker, C., Fransman, W., Wijnhoven, S.W.P., Delmaar, C., et al., 2014. Human exposure to conventional and nanoparticle-containing sprays—a critical review. Environ. Sci. Technol. 48 (10), 5366–5378.
Lovén, K., Isaxon, C., Wierzbicka, A., Gudmundsson, A., 2019. Characterization of airborne particles from cleaning sprays and their corresponding respiratory deposition fractions. J. Occup. Environ. Hyg. 16 (9), 656–667.
Manigrasso, M., Buonanno, G., Fuoco, F.C., Stabile, L., Avino, P., 2015. Aerosol deposition doses in the human respiratory tree of electronic cigarette smokers. Environ. Pollut. 196, 257–267.
Miller, F.J., Asgharian, B., Schroeter, J.D., Price, O., 2016. Improvements and additions to the multiple path particle Dosimetry model. J. Aerosol Sci. 99, 14–26.
National Committee on Radiation Protection, 1997. Measurements. Deposition, Retention and Dosimetry of Inhaled Radioactive Substances. Vol. 125. Bethesda, MD, USA: NCRP Report.
Nazarenko, Y., Lioy, P.J., Mainelis, G., 2014. Quantitative assessment of inhalation exposure and deposited dose of aerosol from nanotechnology-based consumer sprays. Environ. Sci. Nano 1 (2), 161.
NIOSH, 2014. Current Strategies for Engineering Controls in Nanomaterial Production and Downstream Handling Processes. NIOSH, Cincinnati, USA.
Nørgaard, A.W., Jensen, K.A., Janfelt, C., Lauritsen, F.R., Clausen, P.A., Wolkoff, P., 2009. Release of VOCs and particles during use of nanofilm spray products. Environ. Sci. Technol. 43 (20), 7824–7830.
Nuyttens, D., Baetens, K., De Schampheleire, M., Sonck, B., 2007. Effect of nozzle type, size and pressure on spray droplet characteristics. Biosyst. Eng. 97 (3), 333–345.
Oberdörster, G., Oberdörster, E., Oberdörster, J., 2005. Nanotoxicology: an emerging discipline evolving from studies of ultrafine particles. Environ. Health Perspect. 113 (7), 823–839.
Park, J., Ham, S., Jang, M., Lee, J., Kim, S., Kim, S., et al., 2017. Spatial–temporal dispersion of aerosolized nanoparticles during the use of consumer spray products and estimates of inhalation exposure. Environ. Sci. Technol. 51 (13), 7624–7638.
Park, J., Yoon, C., Lee, K., 2018. Comparison of modeled estimates of inhalation exposure to aerosols during use of consumer spray products. Int. J. Hyg Environ. Health 221 (6), 941–950.
Park, J., Ham, S., Kim, S., Jang, M., Lee, J., Kim, S., et al., 2020. Physicochemical characteristics of colloidal nanomaterial suspensions and aerosolized particulates from nano-enabled consumer spray products. Indoor Air 30 (5), 925–941.
Pearce, K., Goldsmith, W.T., Greenwald, R., Yang, C., Mainelis, G., Wright, C., 2019. Characterization of an aerosol generation system to assess inhalation risks of aerosolized nano-enabled consumer products. Inhal. Toxicol. 31 (9–10), 357–367.

Quadros, M.E., Marr, L.C., 2011. Silver nanoparticles and total aerosols emitted by nanotechnology-related consumer spray products. Environ. Sci. Technol. 45 (24), 10713–10719.
Rossi, E.M., Pylkkänen, L., Koivisto, A.J., Nykäsenoja, H., Wolff, H., Savolainen, K., et al., 2010. Inhalation exposure to nanosized and fine TiO2 particles inhibits features of allergic asthma in a murine model. Part. Fibre Toxicol. 7 (1), 35.
Rovelli, S., Cattaneo, A., Nischkauer, W., Borghi, F., Spinazzè, A., Keller, M., et al., 2020. Toxic trace metals in size-segregated fine particulate matter: mass concentration, respiratory deposition, and risk assessment. Environ. Pollut. 266, 115242.
Saber, A.T., Lamson, J.S., Jacobsen, N.R., Ravn-Haren, G., Hougaard, K.S., Nyendi, A.N., et al., 2013. Particle-induced pulmonary acute phase response correlates with neutrophil influx linking inhaled particles and cardiovascular risk. Morty RE, editor. PLoS One 8 (7), e69020.
Schiller, ChF., Gebhart, J., Heyder, J., Rudolf, G., Stahlhofen, W., 1986. Factors influencing total deposition of ultrafine aerosol particles in the human respiratory tract. J. Aerosol Sci. 17 (3), 328–332.
Schiller, ChF., Gebhart, J., Heyder, J., Rudolf, G., Stahlhofen, W., 1988. Deposition of monodisperse insoluble aerosol particles in the 0.005 to 0.2 μm size range within the human respiratory tract. In: Inhaled Particles VI [Internet]. Elsevier, pp. 41–49 [cited 2024 Dec 12]. https://linkinghub.elsevier.com/retrieve/pii/B9780080341859500103.
Smith, S., Cheng, Y.S., Yeh, H.C., 2001. Deposition of ultrafine particles in human tracheobronchial airways of adults and children. Aerosol. Sci. Technol. 35 (3), 697–709.
Son, Y., Mainelis, G., Delnevo, C., Wackowski, O.A., Schwander, S., Meng, Q., 2020. Investigating E-cigarette particle emissions and human airway depositions under various E-cigarette-use conditions. Chem. Res. Toxicol. 33 (2), 343–352.
Sosnowski, T.R., Kramek-Romanowska, K., 2016. Predicted deposition of E-cigarette aerosol in the human lungs. J. Aerosol Med. Pulm. Drug Deliv. 29 (3), 299–309.
Storey-Bishoff, J., Noga, M., Finlay, W.H., 2008. Deposition of micrometer-sized aerosol particles in infant nasal airway replicas. J. Aerosol Sci. 39 (12), 1055–1065.
Su, W.C., Cheng, Y.S., 2006. Fiber deposition pattern in two human respiratory tract replicas. Inhal. Toxicol. 18 (10), 749–760.
Su, W.C., Cheng, Y.S., 2015. Estimation of carbon nanotubes deposition in a human respiratory tract replica. J. Aerosol Sci. 79, 72–85.
Su, W.C., Chen, Y., Xi, J., 2019. A new approach to estimate ultrafine particle respiratory deposition. Inhal. Toxicol. 31 (1), 35–43.
Su, W.C., Wong, S., Buu, A., 2021a. Deposition of E-cigarette aerosol in human airways through passive vaping. Indoor Air 31 (2), 348–356.
Su, W.C., Lin, Y.H., Wong, S.W., Chen, J.Y., Lee, J., Buu, A., 2021b. Estimation of the dose of electronic cigarette chemicals deposited in human airways through passive vaping. J. Expo. Sci. Environ. Epidemiol. 31 (6), 1008–1016.
Su, W.C., Lee, J., Afshar, M., Zhang, K., Han, I., 2024. Assessing community health risks from exposure to ultrafine particles containing transition metals in the Greater Houston Area. Sci. Total Environ. 912, 169067.
Tian, G., Hindle, M., Lee, S., Longest, P.W., 2015. Validating CFD predictions of pharmaceutical aerosol deposition with in vivo data. Pharm. Res. 32 (10), 3170–3187.
U.S. EPA, 1999. Compendium of Methods for the Determination of Inorganic Compounds in Ambient Air [Internet]. EPA. Available from: https://www.epa.gov/sites/default/files/2019-11/documents/overvw3.pdf.
U.S. EPA, 2011. Exposure Factors Handbook, 2011 edition. National Center for Environmental Assessment, Washington (DC), USA.
Verbanck, S., Ghorbaniasl, G., Biddiscombe, M.F., Dragojlovic, D., Ricks, N., Lacor, C., et al., 2016. Inhaled aerosol distribution in human airways: a scintigraphy-guided study in a 3D printed model. J. Aerosol Med. Pulm. Drug Deliv. 29 (6), 525–533.
Voliotis, A., Bezantakos, S., Besis, A., Shao, Y., Samara, C., 2021. Mass dose rates of particle-bound organic pollutants in the human respiratory tract: implications for inhalation exposure and risk estimations. Int. J. Hyg Environ. Health 234, 113710.
Wang, S., Yan, Q., Zhang, R., Jiang, N., Yin, S., Ye, H., 2019. Size-fractionated particulate elements in an inland city of China: deposition flux in human respiratory, health risks, source apportionment, and dry deposition. Environ. Pollut. 247, 515–523.
Wang, W.M., Chen, C.Y., Lu, T.H., Yang, Y.F., Liao, C.M., 2021. Estimates of lung burden risk associated with long-term exposure to TiO2 nanoparticles as a UV-filter in sprays. Environ. Sci. Pollut. Res. 28 (25), 32460–32474.
Zhou, Y., Cheng, Y.S., 2005. Particle deposition in a cast of human tracheobronchial airways. Aerosol. Sci. Technol. 39 (6), 492–500.
Zhou, Y., Xi, J., Simpson, J., Irshad, H., Cheng, Y.S., 2013. Aerosol deposition in a nasopharyngolaryngeal replica of a 5-year-old child. Aerosol. Sci. Technol. 47 (3), 275–282.